Enhanced rock weathering increased soil phosphorus availability and altered root phosphorus-acquisition strategies

Global Change Biology

Bi, Boyuan; Li, Guochen; Goll, Daniel S.; Lin, Luxiang; Chen, Hui et al

https://doi.org/10.1111/gcb.17310

Received: 18 December 2023 | Revised: 1 April 2024 | Accepted: 9 April 2024

DOI: 10.1111/gcb.17310

Global Change Biology WILEY

RESEARCH ARTICLE

Enhanced rock weathering increased soil phosphorus availability and altered root phosphorus-acquisition strategies

Boyuan Bi[1] | Guochen Li[2] | Daniel S. Goll[3,4] | Luxiang Lin[5] | Hui Chen[6] | Tongtong Xu[1] | Qiong Chen[1] | Chenlu Li[7] | Xing Wang[8] | Zhanqing Hao[1] | Yunting Fang[2] | Zuoqiang Yuan[1] | Hans Lambers[9]

[1]Shaanxi Key Laboratory of Qinling Ecological Intelligent Monitoring and Protection, School of Ecology and Environment, Northwestern Polytechnical University, Xi'an, China

[2]CAS Key Laboratory of Forest Ecology and Management, Institute of Applied Ecology, Chinese Academy of Sciences, Shenyang, China

[3]Institute of Geography, University of Augsburg, Augsburg, Germany

[4]Laboratoire Des Sciences du Climat et de l'Environnement, Université Paris-Saclay, Paris, France

[5]CAS Key Laboratory of Tropical Forest Ecology, Xishuangbanna Tropical Botanical Garden, Chinese Academy of Sciences, Kunming, China

[6]National Forest Ecosystem Research Station at Xishuangbanna, Mengla, China

[7]Institute of Interdisciplinary and Innovation Research, Xi'an University of Architecture and Technology, Xi'an, China

[8]Plant Ecology and Nature Conservation, Wageningen University and Research, Wageningen, The Netherlands

[9]School of Biological Sciences and Institute of Agriculture, The University of Western Australia, Perth, Western Australia, Australia

Correspondence
Zuoqiang Yuan, Shaanxi Key Laboratory of Qinling Ecological Intelligent Monitoring and Protection, School of Ecology and Environment, Northwestern Polytechnical University, Xi'an, China.
Email: zqyuan@nwpu.edu.cn

Funding information
Natural Science Basic Research Program of Shaanxi Province, Grant/Award Number: 22JHQ036; Strategic Priority Research Program of the Chinese Academy of Sciences, Grant/Award Number: XDA28020300; Key Research and Development Projects of Shaanxi Province, Grant/Award Number: 2024SF-YBXM-551 and 2024SF-YBXM-558; Key Research and Development Program of Yunnan Province, Grant/Award Number: 202303AC100009; China Postdoctoral Science Foundation, Grant/Award Number: 2023M732864 and 2023M732865; National Natural Science Foundation of China, Grant/Award Number: 32301361, 32171581 and 32230067; Fundamental Research Funds for the Central Universities

Abstract

Enhanced rock weathering (ERW) has been proposed as a measure to enhance the carbon (C)-sequestration potential and fertility of soils. The effects of this practice on the soil phosphorus (P) pools and the general mechanisms affecting microbial P cycling, as well as plant P uptake are not well understood. Here, the impact of ERW on soil P availability and microbial P cycling functional groups and root P-acquisition traits were explored through a 2-year wollastonite field addition experiment in a tropical rubber plantation. The results show that ERW significantly increased soil microbial carbon-use efficiency and total P concentrations and indirectly increased soil P availability by enhancing organic P mobilization and mineralization of rhizosheath carboxylates and phosphatase, respectively. Also, ERW stimulated the activities of P-solubilizing (*gcd*, *ppa* and *ppx*) and mineralizing enzymes (*phoADN* and *phnAPHLFXIM*), thus contributing to the inorganic P solubilization and organic P mineralization. Accompanying the increase in soil P availability, the P-acquisition strategy of the rubber fine roots changed from do-it-yourself acquisition by roots to dependence on mycorrhizal collaboration and the release of root exudates. In addition, the direct effects of ERW on root P-acquisition traits (such as root diameter, specific root length, and mycorrhizal colonization rate) may also be related to changes in the pattern of belowground carbon investments in plants. Our study provides a new insight that ERW increases carbon-sequestration potential and P availability in tropical forests and profoundly affects belowground plant resource-use strategies.

KEYWORDS
carbon-sequestration potential, enhanced rock weathering, phosphorus-acquisition strategy, soil phosphorus availability, wollastonite addition

1 | INTRODUCTION

Climate warming is one of the main environmental challenges currently impacting humanity, and it is inextricably linked to the increasing concentration of carbon dioxide (CO_2) in the atmosphere (IPCC, 2018). Recently, scientists have proposed a series of technologies to absorb atmospheric CO_2 to mitigate negative effects of global warming (Beerling et al., 2018, 2020). Observations by Beerling et al. (2020) suggest that enhanced rock weathering (ERW) can effectively remove CO_2 from the atmosphere and store it in the soil. Specifically, ERW is achieved by adding powdered silicate rock (e.g., wollastonite, basalt, and olivine) to the soil surface, where silicate particles react chemically with dissolved CO_2 to form bicarbonate ions (Smith et al., 2016, 2019). These ions can be transported by rivers to the ocean, where they have the potential to be stored for thousands of years or longer, depending on the calcium carbonate sedimentation process (Peña-Ramírez et al., 2009; Renforth & Henderson, 2017). To date, ERW practices have been used mainly in agriculture, less in forestry, and occasionally in natural ecosystems and ecosystems undergoing restoration (Beerling et al., 2018; Haque et al., 2019).

In tropical or subtropical forests, low availability of rock-derived nutrients like phosphorus (P) (Du et al., 2020; Vitousek et al., 2010) may constrains the positive effects of elevated CO_2 on tree biomass production (Terrer et al., 2019) and may affect microbial processes in the soil (Hou et al., 2018). It can affect both above- and belowground carbon (C)-sequestration potential. He et al. (2023) reported a strongly negative correlation between microbial C-use efficiency (CUE) and microbial metabolic P restriction, which was particularly pronounced in temperate grassland ecosystems. The microbial CUE is also a major driver of soil organic carbon (SOC) variation globally with higher CUE leading to potentially higher SOC (Tao et al., 2023). Therefore, microbial CUE and its C-sequestration effects are inextricably linked to soil P pools. On the other hand, ERW can affect the P availability to plants and soil microbes by releasing P contained in the added minerals, changes in soil pH, microbial CUE, and phosphatase activity. Modeling studies suggest a significant P-mediated effect of ERW (Goll et al., 2021), but it remains to be tested in field trials. Thus, there is a fundamental question: can ERW increase soil P availability by enhancing soil microbial CUE? Clear evidence for this is currently lacking.

Biochemical transformations between soil inorganic and organic P fractions strongly influence P availability and plant P uptake in P-impoverished areas. These transformations include weathering, mineralization, sorption, and solubilization processes (Hou et al., 2016, 2018; Vitousek et al., 2010). Phosphorus in the soil solution, which occurs in very low concentrations (<10 μM; Lambers, 2022; Parfitt, 1979), is the only source of soil P that is readily available to plants, and the replenishment of other components (especially moderately-soluble P) becomes particularly important when it is depleted (Lambers, 2022). By clarifying the soil P components and the microbial transformation processes (e.g., organic P mineralization and inorganic P solubilization and adsorption, etc.) among these fractions, it contributes to our understanding of the dynamics of the soil P pool and its availability in time (Dai et al., 2019). A typical gene involved in solubilizing inorganic P is the gene (*gcd*) coding for quinoprotein glucose dehydrogenase. It directly governs the oxidation pathway of glucose and acidification of the periplasmic space (Elias et al., 2001). In addition, microorganisms containing genes coding for enzymes, such as alkaline phosphatase (*phoD* and *phoA*), phytase (*appA*), and C-P lyases (*phn*), have a high capacities to mineralize organic P compounds in soil (Rodríguez et al., 2006). Therefore, by linking soil microbial CUE with P-pool transformation and its underpinning microbial processes, we can clarify how ERW further affects soil P pool dynamics and its availability by enhancing soil C sequestration.

Phosphorus uptake by plant roots and root acquisition strategies are normally characterized by using root P-acquisition traits (Bi et al., 2023). These traits typically include mycorrhizal colonization rate, specific root length (SRL), root diameter (RD) and rhizosheath phosphatases and carboxylates. Apart from the active uptake of inorganic P by fine roots and hyphae of mycorrhizal fungi, the mobilization and mineralization of organic P by carboxylates and phosphatases secreted by the roots is the most efficient way for plants to acquire P (Lambers, 2022). In fact, at very low P availability, the arbuscular mycorrhizal symbiosis is typically suppressed (Abbott et al., 1984; Treseder & Allen, 2002). Further evidence supports the contention that P-mining strategies may be more effective than P-scavenging strategies at extremely low soil P availabilities (Lambers, Clode, et al., 2015; Lambers, Hayes, et al., 2015; Parfitt, 1979). The first axis of the recently proposed multidimensional root economic space framework more explicitly classifies root P-acquisition strategies into "do-it-yourself" (allocating carbon to fine roots, with low RD and high SRL) and "outsourcing" (allocating C to mycorrhizal partners with high RD and mycorrhizal colonization rate) (Bergmann et al., 2020). Currently, although studies have incorporated rhizosheath phosphatase and carboxylate (or foliar manganese), as well as the aforementioned root P-acquisition traits, into this multidimensional root economic space framework (Han et al., 2022; Wen et al., 2019, 2022), the potential impact of ERW on the P-acquisition strategies of plant roots is not well understood.

Considering the above uncertainties, we conducted a 2-year field experiment of silicate rock (wollastonite in this study) addition in a tropical rubber (*Hevea brasiliensis*) plantation in southwest China. We tested the following hypotheses: (1) ERW would enhance soil microbial CUE and C sequestration; (2) ERW would increase soil total P concentrations by releasing P contained in the added minerals, and

enhance P availability mainly based on indirect effects, i.e. by affecting root P-acquisition traits (such as carboxylates and phosphatases released by roots) and microbial P cycling (such as inorganic P solubilization, organic P mineralization); (3) Silicon or other minerals in ERW may enhance rubber growth (Abd Hadi et al., 2022) and thus the demand for P beyond what scavenging fine roots can provide, so the plant P-acquisition strategy shifts towards reliance on mycorrhizal collaboration.

2 | MATERIALS AND METHODS

2.1 | Study sites and experimental design

The field experiment was conducted in the rubber plantation of Xishuangbanna Botanical Garden, Chinese Academy of Sciences, located in southwestern China (21°33′ N, 101°28′ E, 880–950 m a.s.l.). It has a typical tropical monsoon climate. The average annual temperature is 21.9°C and the average annual precipitation is 1528 mm, which mainly occurs during the growing season from May to October. The rubber plantation was planted in 1994 and the planted area is about 25 ha. The soil type is classified as acidic Oxisol according to the USDA soil taxonomy. The forest soil average pH_{H_2O} was 4.9, and total P was 432.19 mg kg^{-1}.

The silicate rock selected for this study was wollastonite due to its high dissolution rate (Haque et al., 2019). The wollastonite mineral in this study was sourced from Diaobing Mountain, Liaoning, China. To analyze the mineral composition of the crystallized phases within, the rock was pre-ground and sieved to <90 μm, then spiked with 20 wt% Al_2O_3 and manually ground finely in an agate mortar in acetone before analysis via X-ray diffraction (XRD) and X-ray Fluorescence (XRF). Powder XRD analysis was carried out with a Malvern Panalytical Empyrean Series 3 diffractometer using CoKa radiation. XRF analysis was carried out using a spectrometer based on an Rh anode X-ray tube, with X-ray spectra detection through an Amptek® X-123SDD complete spectrometer (Bedford, MA, USA). Phase analysis by XRD showed that calcium metasilicate ($CaSiO_3$, 69.4%) is the main mineral of the wollastonite, other mineral were silicon dioxide (SiO_2, 14.8%), $Ca_6Si_6O_{17}(OH)_2$ (13.1%) and calcium carbonate ($CaCO_3$, 2.6%). The main chemical composition of wollastonite (molten state) by XRF analysis includes 30.36% calcium (Ca), 24.29% silicon (Si), 10.08% manganese (Mn), 1.08% titanium (Ti), 0.16% iron (Fe), 0.12% magnesium (Mg), 0.10% phosphorus (P) and 0.08% sodium (Na).

In April 2021, a wollastonite-addition field experiment was conducted in a rubber plantation based on a latin-square design (Figure S1). There were nine sample plots (20 m × 20 m for each plot) and a 20 m separation between each two plots. This experiment included three wollastonite application rates: control (no wollastonite addition, $n = 3$), low wollastonite addition (2.5 t ha^{-1}, equivalent to 0.25 kg m^{-2}, $n = 3$) and high wollastonite addition (5 t ha^{-1}, equivalent to 0.5 kg m^{-2}, $n = 3$). Wollastonite powder was uniformly sprayed onto the forest floor once by means of broadcasting, whereas no substance was added to the control plots. Among these nine plots, three plots were randomly selected as the control, low, and high wollastonite addition plots, respectively. The wollastonite application rates in this study were determined based on its CO_2 removal mass and its application costs. These costs include the economic costs of mining, crushing, and grinding wollastonite and applying wollastonite on target area. On a regional scale (application area not less than 2×10^6 km^2), an application rate of 0.1 kg m^{-2} can remove about 0.2 Gt CO_2 per year with an average cost of only US$79 per t CO_2. For the same application area, an application rate exceeding 0.5 kg m^{-2} may approximately remove 0.8 Gt CO_2 (less than the expected value of 1 Gt), but with an average cost exceeding US$500 per t CO_2. Therefore, an application rate of about 0.01–0.50 kg m^{-2} may be the most cost-effective application option.

2.2 | Plant and soil sampling

In April 2023, plant and soil samples were collected from all nine plots in the rubber plantation. For each plot, three individual rubber trees were randomly selected. All of these individuals surveyed have a diameter at breast height ranging from 28 to 32 cm and a tree height ranging from 18 to 22 m. We then investigated their root biomass (see Section 3.4 for details). The fine roots were sampled using the root-tracking method, i.e. by searching for the coarse roots of the target stem and looking for the fine root branches growing along the coarse roots (Iversen, 2014; Pregitzer et al., 2002). The fine roots were carefully removed in a 0–20 cm soil profile and gently shaken and used to collect the loosely adhering soil around the root system (considered as bulk soil) and the soil tightly adhering to the surface of the fine roots (<5 mm) was considered as rhizosheath soil. Thus, three rhizosheath soils, three bulk soils, and three root samples were obtained in each plot, respectively. Soil samples were divided into two parts: one part was used for the determination of routine physicochemical properties and the other part was stored frozen (−80°C) for DNA extraction. Soil samples for DNA extraction were obtained by thoroughly mixing of three rhizosheath or bulk soil samples from each plot, respectively ($n = 9$ for rhizosheath and bulk soils, respectively). Simultaneously, 8–10 pieces of intact mature leaves were taken from each individual. The leaves samples were rinsed with deionised water, and dried in an oven at 85°C until constant weight, then the samples were ground in a grinder and finally passed through a 100-mesh sieve. In addition, the collected root samples were divided into two parts: one part was used for determination of root morphology and root nutrients, and the second was stored frozen (−20°C) for determination of mycorrhizal colonization rate and root phosphatase activity.

2.3 | P sequential fraction

The chemical composition (i.e. fraction) of soil P can be divided into inorganic P (P_i), organic P (P_o), secondary and mineral P, and

occluded P according to P availability (Dai et al., 2019). To sequentially extract the chemically specified P fractions in soil and their utilization efficiency, we adopted Hedley's sequential extraction scheme (Hedley et al., 1982), acknowledging the pitfalls associated with this method (Barrow et al., 2021). Briefly, 0.5 g of soil sample was first extracted using anion exchange resin to obtain resin-P, followed by taking 0.5 M $NaHCO_3$ to obtain $NaHCO_3$-P_i and $NaHCO_3$-P_o, then ultrasonicated using 0.1 M NaOH to extract NaOH-P_i and NaOH-P_o, and finally extracted using 1 M HCl to obtain HCl_{dill}-P. After centrifugation and filtration, the supernatant was divided into two groups, and the soil was digested with 10 mL of concentrated HCl for 10 min at 80°C to extract HCl_{conc}-P_i and HCl_{conc}-P_o. Finally, the residual soil was digested with 10 mL of concentrated H_2SO_4 and P-free H_2O_2 at 360°C to extract residual P. These P fractions were further classified into five P pools: plant-available P (resin-P and $NaHCO_3$-P_i), P_o ($NaHCO_3$-P_o and NaOH-P_o), secondary mineral P (NaOH-P_i), primary mineral P (HCl_{dill}-P_i), and occluded P (HClconc-P_i, HClconc-P_o, and residual P) (Figure S2).

2.4 | P-acquisition traits

The Sequential soil-coring method was used to estimate fine root biomass (Li et al., 2020). Specifically, four soil cores at a depth of 10 cm were collected from each plot using a soil auger (inner diameter 5 cm). The living fine roots were picked from the auger and washed with distilled water, dried at 65°C for 72 h and weighed. Fine root biomass was calculated as the mean value of fine root biomass for each treatment of each plot.

Rinsed fine roots were morphologically scanned using a root scanner (400 dpi resolution, DS-6500; Seiko Epson, Nagano, Japan), and total root length, total root surface area, total root volume, RD, and root tip number were measured using the WinRHIZOPro root analysis program (v.2004a; Regent Instruments, Inc., Québec City, QC, Canada). Finally, fine roots were dried to constant weight to obtain root dry mass. SRL was obtained by dividing the total root length by the root dry mass. Specific root surface area (SRA) was obtained by dividing the total root surface area by the root dry mass, and root tissue density (RTD) was obtained by dividing the root dry mass by the total root volume Root branching intensity was obtained by dividing the number of root tips by the total root length.

Mycorrhizal colonization rate was observed by acidic magenta combined with microscopic observation (Trouvelot & Kough, 1986). The rinsed fine roots were cut into 1 cm root segments (about 20–30 segments), immersed in 10% (w/v) KOH solution and kept in a water bath at 85°C for 50 min. The alkaline solution was rinsed and acidified by adding 2% (v/v) HCl solution for 5 min, followed by addition of 0.05% trillium blue stain and water bath at 90°C for 30 min. The stain was rinsed and decolored with 1.8 mL glycerol lactate solution. Finally, all root segments were placed under a 10×20 dissecting microscope for observation of mycorrhizal colonization rate the using grid line intersection technique (Trouvelot & Kough, 1986).

In our study, root phosphomonoesterase activity (RPA, EC 3.1.3.1) was used to represent the activity of root phosphatases, because it is the predominant phosphatase synthesized by plants and microbes (Turner, 2008). RPA was determined using umbelliferon (MUB) as substrate. Briefly, 1 g of fresh root sample was taken and extracted with 125 mL of acetate buffer for RPA. The mixture was stirred with a magnetic stirrer for 5 min and then left to stand for 30 min. 0.2 mL of supernatant was taken in a 96 microtiter plate and the substrate was added, then the microtiter plate was incubated at a constant temperature of 20°C for 4 h. Finally, we measured the amount of fluorescence at 360 nm excitation and 460 nm emission using a multifunctional enzyme marker (Synergy 2; Biotek, Winooski, VT, USA). Afterwards, root samples were dried at 65°C until a constant weight was reached. The unit of RPA was expressed in $\mu mol\, g^{-1} min^{-1}$.

Manganese concentration ([Mn]) in mature leaves can be used as an easily measurable proxy for the assessment of belowground carboxylate-releasing processes in plants grown under low P (Lambers, 2022; Lambers, Clode, et al., 2015; Lambers, Hayes, et al., 2015; Pang et al., 2018). Specifically, 100 mg of milled leaves were digested using a hot concentrated nitric-perchloric (3:1) acid mixture. Leaf [Mn] concentrations were determined by an inductively coupled plasma optical emission spectrometer model 5300DV (Perkin Elmer, Shelton, CT, USA).

Root total C and nitrogen (N) concentrations were determined using an automated elemental analyzer (Vario EL III; Elementar, Hanau, Germany). Root total P concentration was digested by H_2SO_4–H_2O_2, and then determined by a Mo–Sb colorimetric method.

2.5 | Soil microbial CUE

Microbial CUE was assessed using the updated biogeochemical equilibrium model (Cui et al., 2021; Sinsabaugh & Follstad Shah, 2012). We determined the relevant soil parameters required in this model, i.e. dissolved nutrients (dissolved organic carbon [DOC], dissolved organic N [DON], available P [Olsen P], microbial biomass C [MBC], N, and P) and enzyme activities involved in the C (β-1,4-glucosidase [BG] and β-D-cellobiosidase [CHB]), N (β-1,4-*N*-acetylglucosaminidase [NAG] and L-leucine aminopeptidase [LAP]), P (acid phosphatase [AP]) cycling. Methods for the determination of these parameters can be found in Bi et al. (2022) and Cui et al. (2021).

$$CUE = CUE_{max} \times \left\{ \left(S_{C:N} \times S_{C:N} \right) / \left[\left(K_{C:N} + S_{C:N} \right) \times \left(K_{C:P} + S_{C:P} \right) \right] \right\}^{0.5} \quad (1)$$

$$S_{C:N} = \left(1 / EEA_{C:N} \right) \times \left(B_{C:N} \times L_{C:N} \right) \quad (2)$$

$$S_{C:N} = \left(1 / EEA_{C:P} \right) \times \left(B_{C:P} \times L_{C:P} \right) \quad (3)$$

where $S_{C:N}$ and $S_{C:P}$ is a scaler that represents the extent to which the allocation of extracellular enzyme activities (EEA) offsets the disparity between the elemental composition of available resources and the composition of microbial biomass (Sinsabaugh et al., 2016). $EEA_{C:N}$ was calculated as (BG+CBH)/(NAG+LAP), and $EEA_{C:P}$ was calculated

as (BG+CBH)/AP. Molar C:X ratios of labile substrate were used as estimates of $L_{C:N}$ and $L_{C:P}$. Labile substrate availability for C, N and P was measured as the quantity of DOC, DON and Olsen P. Moreover, $K_{C:N}$ and $K_{C:P}$, which are half-saturation constants for CUE based on C, N, and P availability, were assumed to be 0.5 (Sinsabaugh & Follstad Shah, 2012). The value of CUE_{max} was assigned as 0.6, which is the upper limit for microbial growth efficiency based on thermodynamic constraints (Sinsabaugh et al., 2016).

2.6 | DNA extraction and metagenomic analysis

Metagenomic DNA extraction and Shotgun sequencing were performed using the DNA Kit (D5625-01; OMEGA, USA). Total microbial genomes from 18 DNA samples were extracted and stored frozen prior to further assessment. The quantity and quality of extracted DNA were measured using a NanoDrop ND-1000 spectrophotometer (Thermo Fisher Scientific, Waltham, MA, USA) and agarose gel electrophoresis, respectively. Metagenomic shotgun sequencing libraries with an insert size of 400 bp were constructed using the Illumina TruSeq Nano DNA LT Library Preparation Kit. Each library was sequenced on an Illumina HiSeq X-ten platform (Illumina, USA) using the PE150 strategy at Personal Biotechnology Co. Metagenomic sequence data were uploaded to the NCBI Sequence Read Archive database (accession number: PRJNA1072228). All genes in each sample were functionally annotated and classified by comparison with the KEGG Ontology numbers. Combined with previous studies (Dai et al., 2019; Lu et al., 2022), the genes involved in the P cycle (37 genes were extracted in this study) were mainly involved in four processes: P-starvation response, P transformation, organic P mineralization, and inorganic P solubilization (Table S1).

2.7 | Statistical analyses

Prior to subsequent statistics, we firstly averaged measure values of the three (rhizosheath and bulk) soils properties and plant traits for each plot respectively, thus $n=3$ for each treatment. To investigate the effect of ERW and location (rhizosheath and bulk soil) on soil C (SOC, DOC, MBC), microbial CUE, P fractions and microbial P-cycling functional genes, a linear mixed-effects model was applied using *lmer* function of "lme4" package. In this model, the rows and columns of latin-square blocking were used as random effects, and the wollastonite application rate, location, and their interactions were considered as fixed effects. For the root functional traits (e.g. fine root biomass, RD, SRL and RPA, etc.), the rows and columns of latin-square blocking were also used as random effects, and the wollastonite application rate was considered as a fixed effect. We set wollastonite application rate as a categorical variable (High, low and control). Differences among three application rate treatments or between rhizosheath and bulk soils were tested using the "emmeans" package. Differences among different treatments in the soil C, microbial CUE, P fractions, root functional traits, and microbial P-cycling functional genes were visualized using the "sjPlot" package. Principal component analysis (PCA) was applied to visualize the coordination of root functional traits to determine the expression of P-acquisition traits such as RPA, leaf [Mn] and the distribution of all samples in the root economics spectrum and used to downscale the five soil P fractions and represent the soil P availability by the first component (PC1). PCA was performed using the *prcomp* function in the "factoextra" package. Spearman's correlation analysis was used to determine the correlation between root P-acquisition traits, the visualization of the correlation heatmaps was implemented using the package of "corrplot". Mantel tests were performed to identify correlations among the rhizosheath P availability and microbial CUE, root P-acquisition traits and P-cycling functional genes under ERW condition by using packages of "linkET" and "dplyr". The main predictors for P availability were identified by random forest analysis using package of "randomForest". In this model, soil edaphic factors, root P-acquisition traits, P-cycling functional genes and CUE served as predictors for P availability. The ranking method was based on the percentage increase in mean square error. Finally, a partial least squares pathway modeling (PLS-PM) was performed to determine the indirect and/or direct effects on P availability among the wollastonite additions, soil edaphic factors, root P-acquisition traits, P-cycling functional genes and microbial CUE using the package of "plspm" (Sanchez et al., 2013). All statistical analyses were performed in software R (version 4.1.1).

3 | RESULTS

3.1 | ERW effects on soil edaphic factors, microbial CUE, and fine root biomass

Compared with the control, wollastonite application increased SOC concentrations; the effect on rhizosheath SOC was significant at low application, and on bulk SOC at high application (Figure 1; Tables S2 and S3). Soil dissolved organic C and microbial biomass C concentrations at high wollastonite treatment were higher than those in control in both rhizosheath and bulk soil, and microbial biomass C concentrations in particular were increased by at least 80% compared with the control. In addition, wollastonite addition significantly increased soil microbial CUE in the rhizosheath soil, and the fine root biomass with wollastonite addition was significantly greater than that of the control (Figure 1e).

3.2 | ERW effects on soil P fraction

Soil P availability of the rubber plantation was significantly enhanced by wollastonite addition (Figure 2; Tables S4 and S5). Specifically, available P and secondary mineral P concentrations gradually increased with wollastonite addition in both rhizosheath and bulk soil (Figure 2a,c), while the opposite was true for primary mineral P concentrations (Figure 2d). Soil P_o and occluded P concentrations with

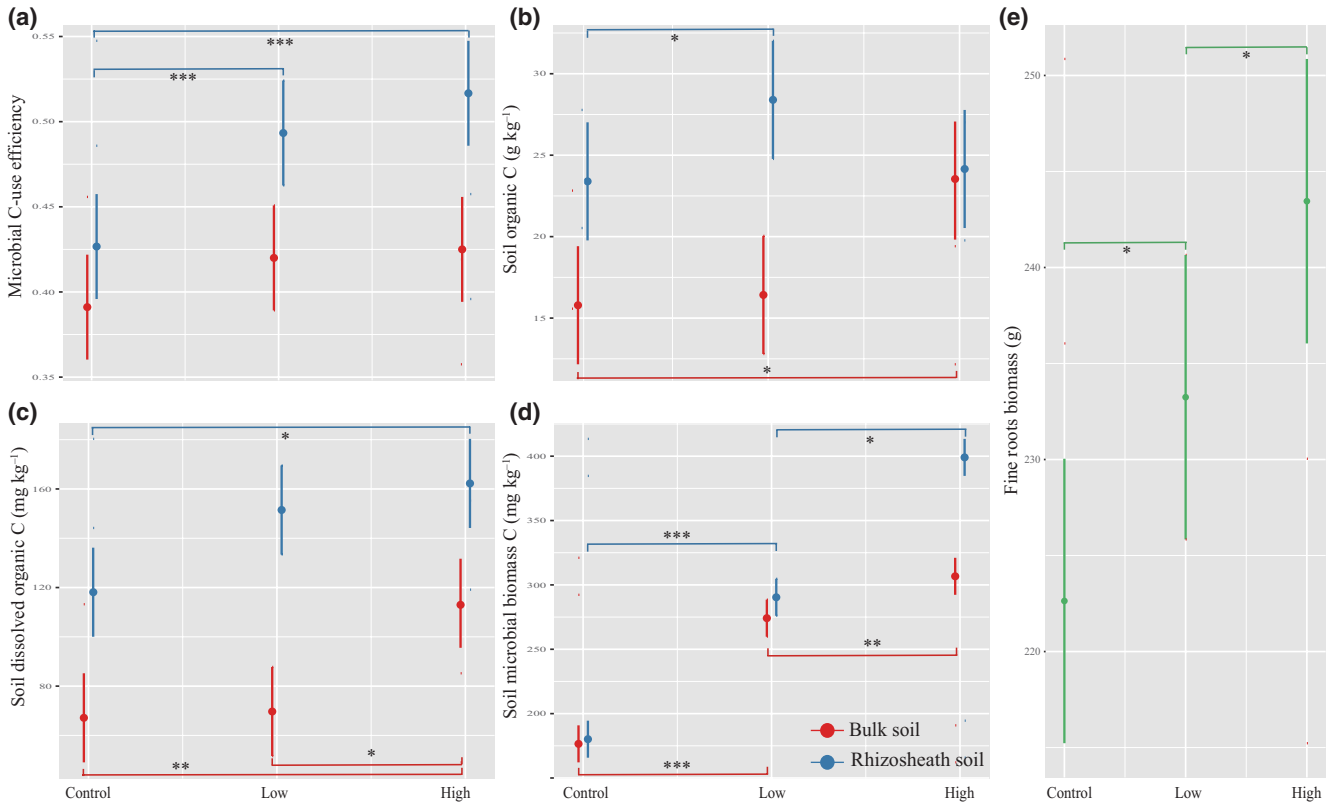

FIGURE 1 The comparisons of soil microbial carbon-use efficiency (a), organic carbon (b), dissolved organic carbon (c), microbial biomass carbon (d) in the rhizosheath and bulk soil, and fine root biomass (e) across the different wollastonite application rates by a linear mixed-effects model. Values and 95% confidence intervals in the figure are derived from a contrast analysis of the model represented in Table S2. Asterisks represent significant differences among wollastonite application treatments in the rhizosheath or bulk soil. Control referred to no wollastonite addition (0 kg m^{-2}, $n = 3$); Low referred to low wollastonite application (0.25 kg m^{-2}, $n = 3$); High referred to high wollastonite application (0.50 kg m^{-2}, $n = 3$). *, $p < .05$; **, $p < .01$; ***, $p < .001$.

high wollastonite addition were significantly greater than those of the control, whereas we found no significant effect in the rhizosheath soil (Figure 2b,e). In both rhizosheath and bulk soils, total P concentrations with high wollastonite addition were significantly greater than those of the control (Figure 2f; Table S4).

3.3 | ERW effects on P-acquisition traits

Root P-acquisition traits responded differently to wollastonite addition (Figure 3). Specifically, root phosphomonoesterase activities, leaf [Mn] and RTD were significantly lower in the control than in the wollastonite treatments ($p < .01$). In contrast, the greatest SRL and root total N concentrations were observed in the control (Figure 3a; Tables S6 and S7). The PCA showed a multidimensional root economics spectrum across three concentrations of wollastonite addition (Figure 3b; Table S8). The samples from the control were generally distributed on the "Do-it-yourself" side of the first axis and the "Fast" side of the second axis, suggesting that rubber trees without wollastonite addition tended to absorb P more through the fine roots, rather than symbioses (with higher SRL and area). The samples from greater wollastonite addition treatments mainly distributed on the "Outsourcing" side of the first axis, and there was a strong positive correlation between mycorrhizal colonization and leaf [Mn] and RPA (Figure 3c), suggesting that rubber trees not only relied on the cooperation with mycorrhizal fungi, but also on root exudates (i.e. enhancing the mobilization and mineralization of P_o) for P uptake. These results imply that wollastonite addition altered the P-acquisition strategy of rubber roots, i.e. from do-it-yourself P uptake by fine roots towards acquisition via mycorrhizal partners and root exudates.

3.4 | ERW effects on P-cycling functional microbes

A total of 37 functional genes involved in P_i solubilization, P_o mineralization, P transport and regulation were detected in the metagenomes, which we used to determine the mechanisms of the microbial involvement in soil P cycling. The results showed a greater abundance of functional genes involved in microbial P_i solubilization and P transport (Figure 4). Three key genes (*ppa*, *ppx*, *gcd*) involved in P_i solubilization were more abundant in both rhizosheath and bulk soils with wollastonite addition ($p < .05$). Most of the P_o mineralization genes (e.g., *appA*, *phoADN*, *phnAPHLFXIM*) and P transport genes (*ugpABCE* and *phnCDE*) in the rhizosheath soil were more abundant at the high wollastonite treatment than in the control (Table S9). The abundance of genes involved in P cycling with wollastonite addition,

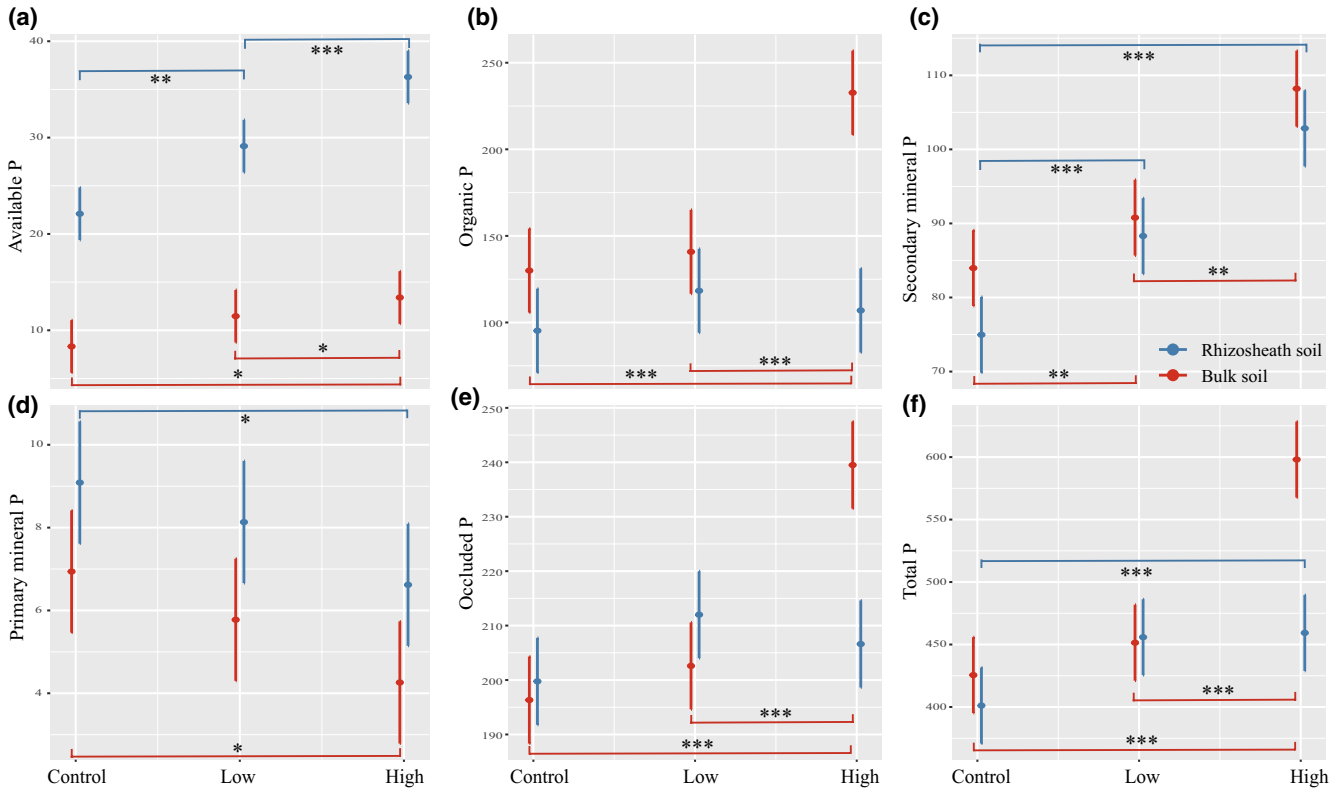

FIGURE 2 The comparisons of soil P fractions (mg kg^{-1}) across the different wollastonite application rates in the rhizosheath and bulk soils by a linear mixed-effects model. (a) Available P, (b) Organic P, (c) Secondary mineral P, (d) Primary mineral P, (e) Occluded P and (f) Total P. Values and 95% confidence intervals in the figure are derived from a contrast analysis of the model represented in Table S4. Asterisks represent significant differences among wollastonite application treatments in the rhizosheath or bulk soil. Control referred to no wollastonite addition (0 kg m^{-2}, $n = 3$); Low referred to low wollastonite application (0.25 kg m^{-2}, $n = 3$); High referred to high wollastonite application (0.50 kg m^{-2}, $n = 3$). *, $p < .05$; **, $p < .01$; ***, $p < .001$.

except for P-starvation response genes, were more abundant than those of the control in the rhizosheath soil (Figure 4).

3.5 | Factors driving P availability

Except for occluded soil P, the other four P fractions showed strong associations with root P-acquisition traits, P-cycling functional genes and microbial CUE (Figure 5a). For example, strong correlations existed between available P and P-acquisition traits (such as RP, RPA, [Mn] and RMC) and microbial P-cycling functional group (such as genes involved in P_i solubilization, P_o mineralization, and P transport). Simultaneously, predictive models (explaining 68.7% of the variation) suggested that the above factors were also the most important drivers affecting P availability (Figure 5b). Furthermore, PLS-PM analyses revealed that the ERW indirectly increased soil P availability mainly by affecting root P-acquisition traits and microbial P-cycling (Figure 5c). However, the effect of microbial CUE was weakened in this model. These results suggest that ERW increased soil P availability by enhancing the release of root exudates (carboxylates and phosphomonoesterase), collaboration among root traits (mycorrhizal colonization and SRL), and microbial P cycling (processes of P_i solubilization and P_o mineralization).

4 | DISCUSSION

Enhanced rock weathering measures are considered for CO_2 removal with potential for additional organic C sequestration potential (Beerling et al., 2020; Goll et al., 2021). An integrated performance modeling approach assessed the large potential for China and other three countries (India, the USA and Brazil) to apply ERW to together remove 0.5–2 Gt of CO_2 per year by 2050, and China's projected increase in low-carbon energy usage allows net CO_2 removal to rise by substantially reducing secondary CO_2 emissions from logistical operations (Beerling et al., 2020; Goll et al., 2021). It should be noted, however, that China's 2022 CO_2 emissions of 15.684 Gt still strongly require economic decarbonization policy interventions, rather than relying solely on ERW. Further reports now emphasize the efficiency and potential of ERW for CO_2 removal, but how this addition affects soil functioning is poorly understood, especially for plantations.

This study showed that ERW significantly increased soil microbial CUE and total P concentration, and enhanced soil P availability by enhancing mobilization and mineralization of plant rhizosheath carboxylates and phosphatase for P_o, and soil microbial P cycling such as P_i solubilization and P_o mineralization. Second, with the

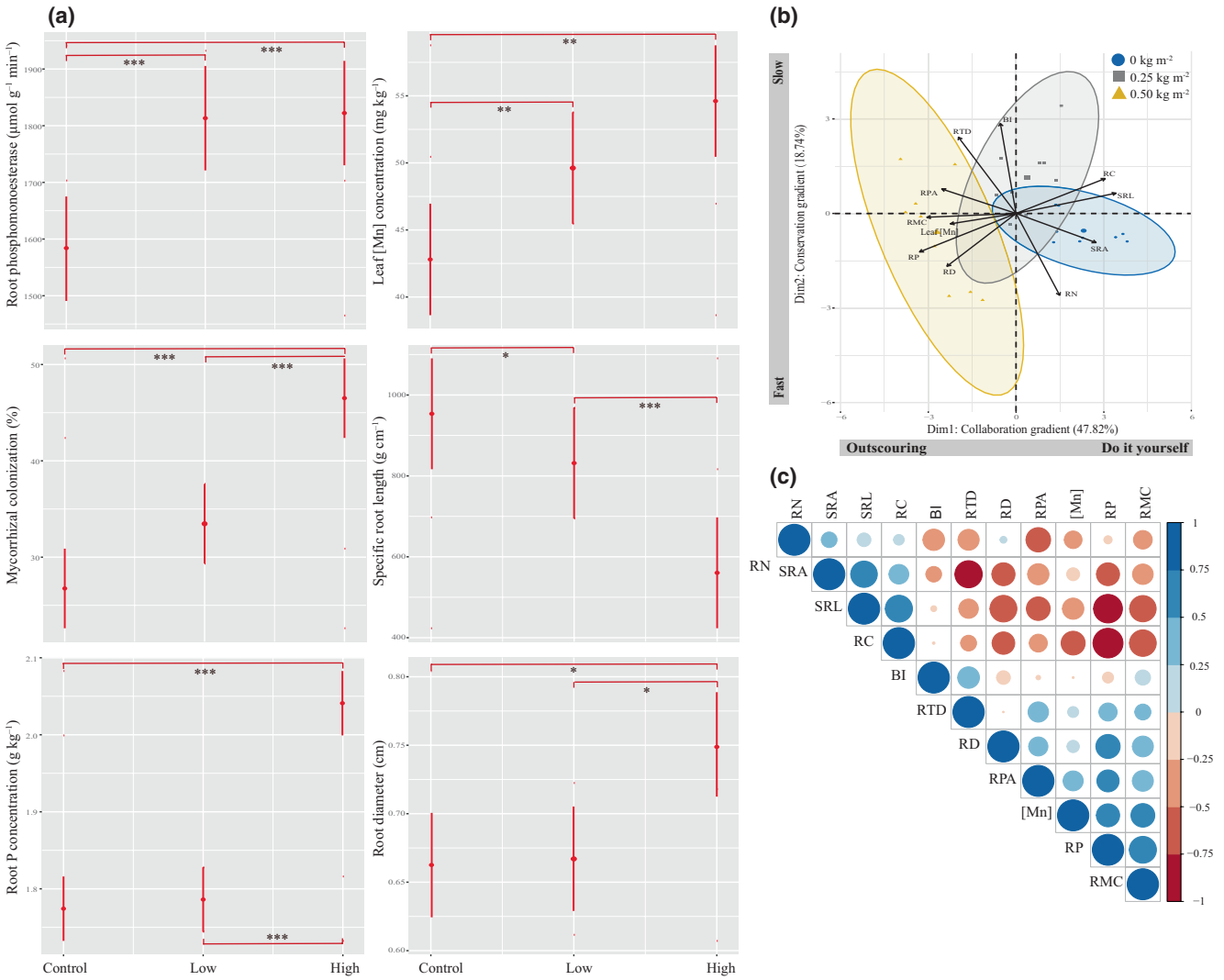

FIGURE 3 Effects of wollastonite addition on root functional traits and phosphorus (P)-acquisition strategies of a rubber plantation. (a) The comparisons of root P-acquisition traits across the different wollastonite application rates by a linear mixed-effects model. Values and 95% confidence intervals in the figure are derived from a contrast analysis of the model represented in Table S6. Asterisks represent significant differences among wollastonite application treatments in the rhizosheath or bulk soil. Control referred to no wollastonite addition (0 kg m^{-2}, $n = 3$); Low referred to low wollastonite application (0.25 kg m^{-2}, $n = 3$); High referred to high wollastonite application (0.50 kg m^{-2}, $n = 3$). (b) Principal component analysis was applied to visualize the coordination of root functional traits to determine the expression of P-acquisition traits such as root phosphomonoesterase and the distribution of all samples in the root economics space. The first axis (collaboration gradient) represents the shift from a "do-it-yourself" soil exploration strategy (higher SRL and SRA) to an "outsourcing" resource strategy (higher mycorrhizal colonization and root diameter) of investing carbon (C) in mycorrhizal partners, and the second axis (conservation gradient) represents the resource return on investment from slow (higher root tissue density, i.e. greater root construction costs, with long-lived roots) to fast (higher root total nitrogen concentration, i.e. faster metabolic rates, with short life span). (c) Heatmap of Spearman's correlations for root functional traits. BI, branching intensity; [Mn], leaf manganese concentration; RC, root total carbon concentration; RD, root diameter; RMC, mycorrhizal colonization rate; RN, root total nitrogen concentration; RP, root total phosphorus concentration; RPA, root phosphomonoesterase activity; RTD, root tissue density; SRA, specific root surface area; SRL, specific root length. *, $p < .05$; **, $p < .01$; ***, $p < .001$.

increase in soil total P concentration, the P-acquisition strategy of the plant shifted from acquisition by fine roots to reliance on collaborative acquisition by mycorrhizal hyphae and root exudates. In the context of rising global CO_2, this study highlights that ERW can indeed alter soil P availability in a tropical plantation with potential for additional organic C sequestration in P-impoverished systems (Figure 6).

4.1 | ERW enhanced soil C-sequestration potential in tropical plantations

This study showed that the SOC concentrations were greater in the high wollastonite addition, especially for the rhizosheath soils ($p < .05$, Figure 1; Table S2). The significant increase in soil microbial CUE by ERW can be, to some extent, also an indication

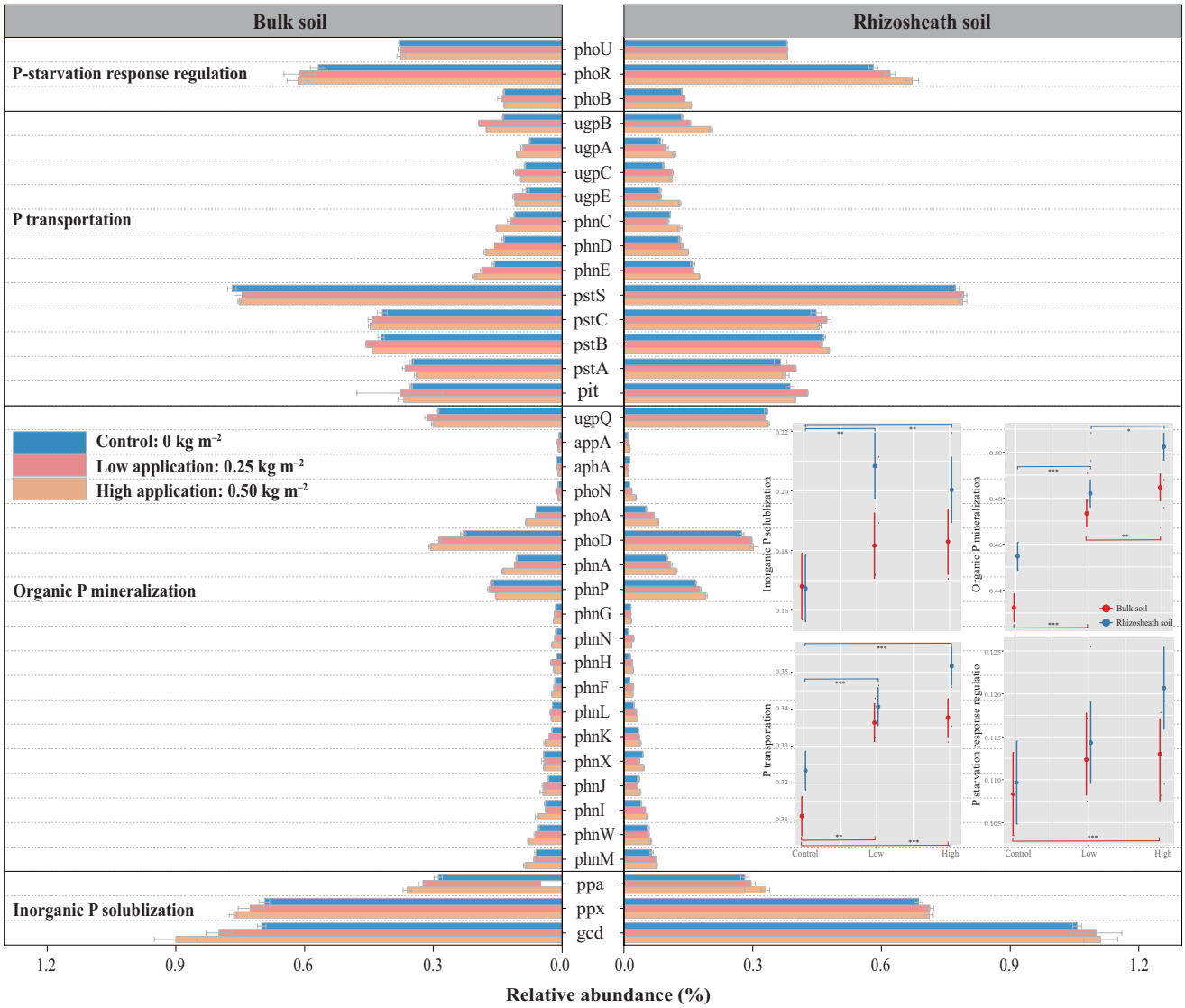

FIGURE 4 The comparisons of microbial functional genes abundance of the phosphorus (P) cycle across the different wollastonite application rates ($n = 3$ for each treatment) in the rhizosheath and bulk soil by a linear mixed-effects model. Values and 95% confidence intervals in the figure are derived from a contrast analysis of the model represented in Table S9. According to the specific function of these genes, they were classified as P-starvation response genes, P transformation, organic P mineralization and inorganic P solubilization. The bottom right panel showed the comparisons among these four functional groups. Asterisks represent significant differences among wollastonite application treatments in the rhizosheath or bulk soil. *, $p < .05$; **, $p < .01$; ***, $p < .001$.

of increased soil C-sequestration potential (Hagerty et al., 2018; Sinsabaugh et al., 2016; Tao et al., 2023). This is because higher CUE values may indicate more efficient conversion of exogenous C into microbial biomass, which equates to greater potential for long-term C sequestration (Manzoni et al., 2012, 2017) and CUE is a major driver of SOC variation, globally (Tao et al., 2023). An experimental study demonstrated the effect of wollastonite on microbial functioning by increasing nutrient access of microbes connected to increasing soil pH, and silicon and P concentrations (Yan et al., 2023). In fact, empirical data on the effect of silicate addition on C sequestration in forest soils are still scarce, so this study provides clear evidence that ERW enhanced C sequestration in tropical plantation soils. In addition to the effects of enhanced CUE on the biological conversion of soil C inputs into stable SOC, powdered silicate rock addition can also affect soil C sequestration by influencing the amount and quality of belowground C inputs by plants and the physical stabilization of soil organic matter (Paradelo et al., 2016).

4.2 | ERW indirectly enhanced soil P availability

Enhanced rock weathering had a positive effect on P availability in the soil which was mainly mediated by plant roots and soil microbial processes (Figure 5b,c). Besides, ERW released P contained in the added minerals, increasing the total P concentration of the soil. The direct effects were mainly based on microbial functional groups affecting soil P_o mineralization and P_i solubilization, and P_o

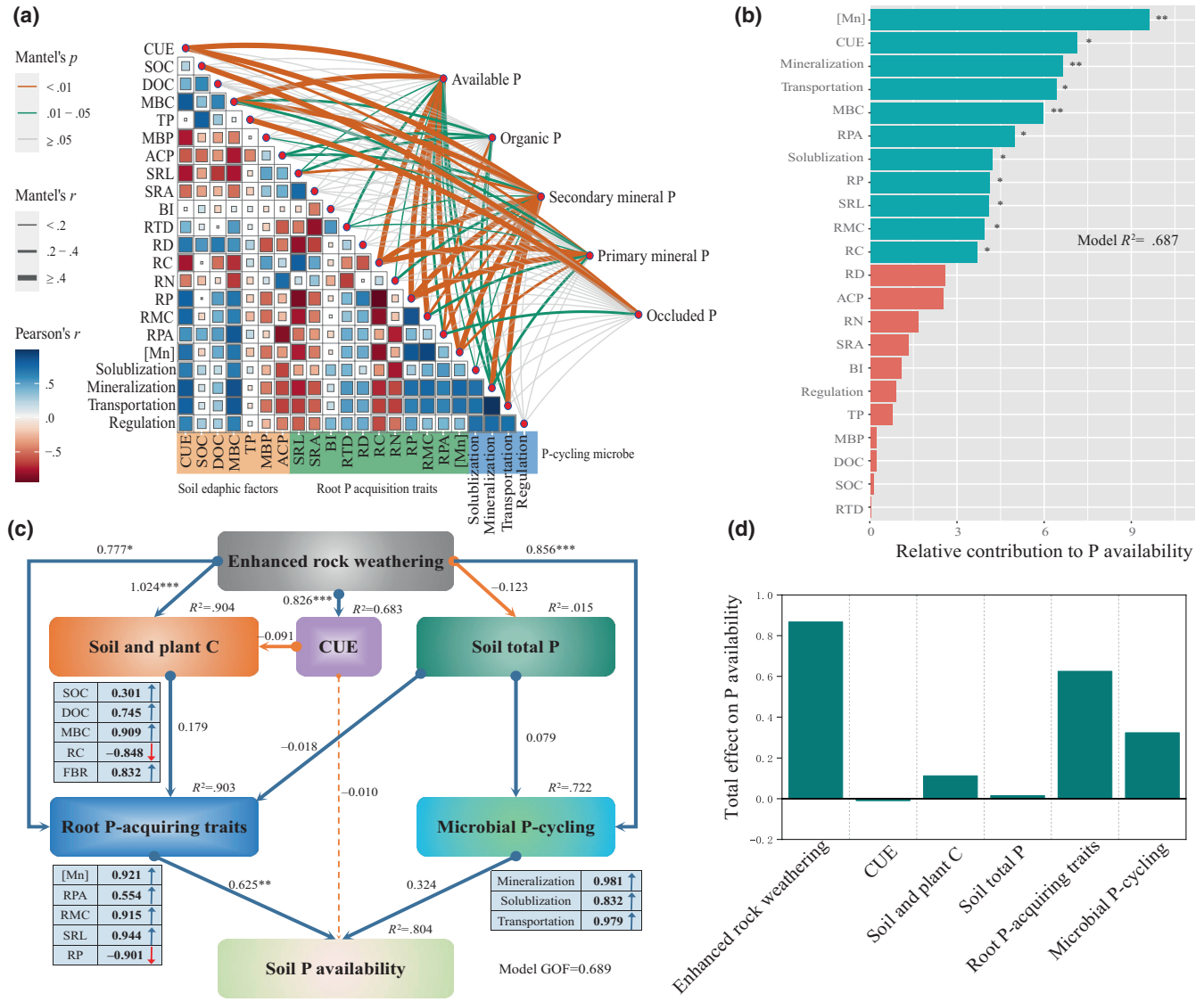

FIGURE 5 Mantel test for the multiple correlations among soil edaphic factors, root phosphorus (P)-acquisition traits, P-cycling functional genes, and microbial carbon-use efficiency effects on soil P availability under wollastonite-addition treatment (a). Relative importance analysis (random forest model) for predicting P availability (b). Blue rectangles represent significant predictors, while red rectangles represent non-significant predictors; the ranking method was based on the percentage increases in mean square error. Here, P availability refers to the first principal component (PC1) after down-scaling the soil P fraction through PCA. Partial least squares pathway modeling (PLS-PM) was performed to determine the indirect and/or direct effects on P availability among enhanced rock weathering, soil carbon and fine root biomass (FRB), microbial C-use efficiency (CUE), root P-acquisition traits and microbial P-cycling (c, d). In this model, the blue line represents a positive effect between two variables, while the orange color represents a negative effect. Significant path coefficients are marked with asterisks: *$p < .05$; **$p < .01$; ***$p < .001$. GOF, goodness-of-fit.

mobilization and mineralization by carboxylates and phosphatase from plant rhizosheath. Our findings were similar to a modeling study, i.e. ERW enhanced background P input and its availability by several orders of magnitude (Goll et al., 2021). Changes in soil microbial functional groups were associated with the addition of silicate rock (Figure 4). In general, microbial taxa shifted towards taxa that are better able to occupy new niches on mineral surfaces or benefit from released nutrients (Reith et al., 2015). Powdered silicates enhance microbial nitrification (Mersi et al., 1992), but reliable data on P cycling were not available. The present study provides new evidence that ERW increases the abundance of functional genes involved in P_i solubilization and P_o mineralization. The reason for this may be that ERW provides microorganisms with more substrate (i.e. C and P) by enhancing microbial CUE and SOC concentrations and releasing P-contained minerals (Figures 1 and 2), stimulating the efficiency of microbial P-cycling functional groups during P-pool conversion and utilization. On the other hand, increased phosphomonoesterase and carboxylates released by plant roots can effectively mineralize and mobilize soil P_o to increase soil P availability (Lambers, 2022; Wen et al., 2019). Thus, ERW could indeed have a positive side-effect of improving P availability as suggested by modeling in P-deprived environments (Goll et al., 2021).

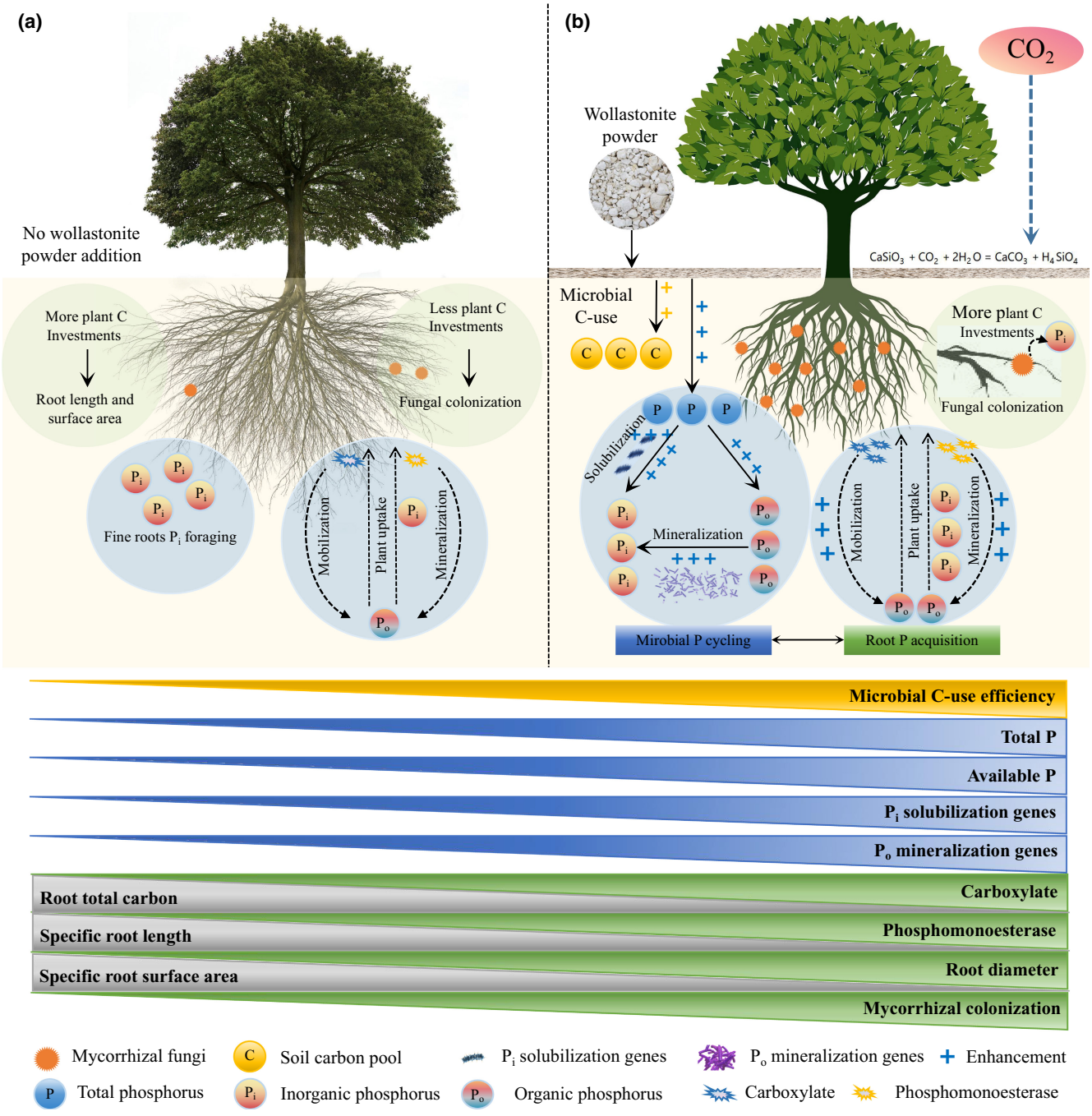

FIGURE 6 Schematic diagram of the effects of enhanced rock weathering on soil phosphorus (P) availability and plant P-acquisition strategies. (a) The scenario when wollastonite was not added. In this case, plants rely more on the exploration of the soil matrix by fine roots to acquire P, and therefore invest more carbon (C) in increasing specific root length and specific surface area. The root system is characterized by fast turnover and short life span. The fine roots also acquire P by solubilizing and mineralizing soil inorganic P via root-secreted carboxylates and phosphatases, respectively. However, efficiency of P acquisition through root exudates was significantly enhanced by the addition of wollastonite. (b) The scenario when wollastonite was added. The basic principle is that the main component of wollastonite ($CaSiO_3$) reacts with CO_2 and water to form a $CaCO_3$ precipitate, which in turn can enhance C sequestration in the soil. As a result, the soil organic C, dissolved organic C, and microbial biomass C increased to different degrees compared with the control, and the efficiency of microbial C utilization was significantly enhanced. Second, the total soil P concentration increased due to the input of P-containing minerals from wollastonite. In this case, the metabolism of P-cycling microorganisms was also gradually enhanced, as reflected by the enhanced P-solubilizing (*gcd*, *ppa* and *ppx*) and mineralizing enzyme activities (*phoADN* and *phnAPHLFXIM*), which increased soil P availability from the soil perspective. Third, as P concentrations increases, the plant P-acquisition strategy of the absorptive roots shifts from reliance on fine roots for inorganic P to mycorrhizal collaboration for P acquisition and enhanced secretion of carboxylates and phosphatases, thereby increasing soil P availability from the plant perspective.

4.3 | Root P-acquisition strategies varied with ERW

Phosphorus acquisition by roots is generally via fine root uptake, releases of root exudates or dependent on mycorrhizal collaboration (Lambers, 2022). However, these acquisition modes are generally antagonistic and strongly dependent on soil P availability (Liu et al., 2021). Incorporating root P-acquisition traits into a multidimensional root economic spectrum allows for a clearer determination of the variation in P-acquisition strategies of absorptive roots and their trade-offs (Bergmann et al., 2020; Bi et al., 2023; Han et al., 2022). Generally, species with fine roots tend to expand their contact surface with the soil more (higher SRL and SRA and small RD) and have more fine-root branches for P acquisition, whereas species with coarse roots rely more on mycorrhizas for nutrient acquisition from the soil (Ma et al., 2018). The results of the study refute the third hypothesis we proposed (i.e. the plant P-acquisition strategy shifts from fines root foraging and carboxylate mobilization towards reliance on mycorrhizal collaboration), because the increase in soil total P concentration due to ERW addition was accompanied by a change in the P-acquisition strategy of the rubber roots, i.e. a gradual shift from acquisition by fine roots to a reliance on collaborative acquisition by mycorrhizal hyphae and the release of root exudates (phosphomonoesterase and carboxylates) (Figure 3). The unexpected finding was a gradual increase of carboxylate secretion. Normally, when soil is extremely P-deprived, plants mobilize soil inorganic P for plant uptake mainly by releasing carboxylates (Lambers, 2022; Wen et al., 2022). The reasons for this may be: (1) silicon and its minerals in rocks may promote plant growth (such as fine root biomass) and hence P demand, which enhanced the release of carboxylates and their mobilization to organic P; (2) even with the addition of P-containing minerals, the total soil P concentration and P availability might still be lower due to soil leaching caused by the high-rainfall environment of tropical forests, so P mobilization by carboxylates would be an effective strategy of P uptake for plants (Lambers, 2022). In addition, the variation in root P-acquisition traits was also directly affected by ERW (Figure 5c). For example, fine root biomass, RD, and RTD were significantly increased following wollastonite addition (Figure 3). This is likely related to the belowground C-investment strategy of plants. Plants tend to allocate more C to mycorrhizal fungi for P uptake rather than for enhancing root length and root surface area under high wollastonite addition (Bi et al., 2023; Ma et al., 2018). Thus, the results of this study shed light on the fact that short-term ERW can change the P-acquisition strategy of plants by increasing total P concentration and its availability.

4.4 | Limitations

Our study revealed that short-term ERW enhanced soil C sequestration and had a positive effect on soil P availability, but some uncertainties remain. First, this study is based on results obtained from 2 years of wollastonite addition, and results might change as times goes on (Beerling et al., 2018). For example, long-term ERW will have a significant effect on soil pH and stoichiometry ratio (such as C:N and N:P), which in turn may inhibit microbial diversity and P-cycling potential (Garcia et al., 2020). Second, dissimilar types of silicate rocks (e.g., basalt and olivine) and their composition may have heterogeneous effects on soil P pool and its availability. The content of P-containing minerals in different silicates may vary considerably, thereby affecting P uptake and utilization by plants. For example, the rocks containing basalt and granite have 1.78% P (Buss et al., 2023), whereas the rocks used in this study has only 0.097% P. Third, a major constraint to fully utilizing ERW for CO_2 removal is the economic cost of mining, crushing and milling silicate and applying silicate powder to forest ecosystems (Goll et al., 2021; Smith et al., 2016). This study used anthropogenic wollastonite addition on a small scale. If scaled up to large-scale application, more economical methods such as spreading silicate powder in the form of free-flowing dust or slurry using a spreader would have to be considered. Regardless, this study provides evidence that wollastonite enhanced P availability and could be used in a tropical plantation to stabilize soils. The wollastonite addition not only save fertilizer costs, but remove considerable amounts of CO_2. Furthermore, the application of ERW in plantations may be much easier and less risky than in natural forest.

5 | CONCLUSION

This study demonstrated that ERW enhanced soil microbial CUE and total P concentration, and enhanced soil P availability by enhancing mobilization and mineralization of plant rhizosheath carboxylates and phosphatase for P_o, and soil P-cycling microbial communities and their associated encoding microbial enzymes involved in P_i solubilization and P_o mineralization. The increase in soil total P concentration and its availability was accompanied by a responsive alteration in the root P-acquisition strategy of a tropical rubber plantation, i.e. a gradual shift from acquisition by fine roots to dependence on collaborative mycorrhizal fungi and the release of root exudates. The results further showed that ERW had a direct effect on plant root P-acquisition traits (e.g., RD, RTD, SRL, and RMC), which may be associated with a shift in the pattern of belowground C-resource partitioning in the plant. Our study elucidates the fact that ERW measures can significantly increase soil P availability in tropical forests and mediate the P-acquisition strategies of roots. Thereby, its application in tropical biomass plantation systems for abiotic CO_2 removal and to stabilize or improve soil fertility should be considered.

AUTHOR CONTRIBUTIONS

Boyuan Bi: Conceptualization; data curation; formal analysis; funding acquisition; investigation; methodology; writing – original draft; writing – review and editing. **Guochen Li:** Formal analysis; methodology; resources. **Daniel S. Goll:** Writing – review and editing. **Luxiang Lin:** Investigation. **Hui Chen:** Investigation. **Tongtong Xu:** Investigation; methodology. **Qiong Chen:** Investigation; methodology. **Chenlu Li:** Investigation; methodology. **Xing**

Wang: Investigation. **Zhanqing Hao:** Supervision. **Yunting Fang:** Supervision. **Zuoqiang Yuan:** Conceptualization; funding acquisition; investigation; methodology; supervision; writing – review and editing. **Hans Lambers:** Supervision; writing – review and editing.

ACKNOWLEDGMENTS

This work was supported by the Strategic Priority Research Program of the Chinese Academy of Sciences (XDA28020300), National Natural Science Foundation of China (32301361, 32171581, 32230067), Natural Science Basic Research Program of Shaanxi (22JHQ036), the China Postdoctoral Science Foundation (2023M732864, 2023M732865), the Key Research and Development Program of Shaanxi (2024SF-YBXM-551, 2024SF-YBXM-558), the Key Research and Development Program of Yunnan Province (202303AC100009) and the Fundamental Research Funds for the Central Universities. We would also appreciate Professor Ziliang Zhang from Northwestern Polytechnical University, and two anonymous reviewers for their careful reviews and valuable comments on this work.

CONFLICT OF INTEREST STATEMENT

The authors declare no competing interests.

DATA AVAILABILITY STATEMENT

The data that support the findings of this study are openly available in figshare at https://doi.org/10.6084/m9.figshare.25688481. Raw sequencing data are additionally deposited at the NCBI Sequence Read Archive (https://www.ncbi.nlm.nih.gov/) under accession number PRJNA1072228.

ORCID

Boyuan Bi https://orcid.org/0000-0002-4996-1115
Daniel S. Goll https://orcid.org/0000-0001-9246-9671
Yunting Fang https://orcid.org/0000-0001-7531-546X
Zuoqiang Yuan https://orcid.org/0000-0001-9197-7076
Hans Lambers https://orcid.org/0000-0002-4118-2272

REFERENCES

Abbott, L. K., Robson, A. D., & De Boer, G. (1984). The effect of phosphorus on the formation of hyphae in soil by the vesicular-arbuscular mycorrhizal fungus *Glomus fasciculatum*. *New Phytologist*, *97*(3), 437–446. https://doi.org/10.1111/j.1469-8137.1984.tb03609.x

Abd Hadi, S. M. H. S., Zakaria, L., Sidique, S. N. M., Mahyudin, M. M., Berahim, Z., Idris, M. A., & Nor, N. M. I. M. (2022). Silicon mediates the changes in physiological performance, nutrient uptake, root colonization morphology and secondary metabolite activity in rubber rootstock seedlings (*Hevea brasiliensis*) inoculated with *Rigidoporus microporus*. *Plant Pathology*, *71*(9), 1956–1968. https://doi.org/10.1111/ppa.13621

Barrow, N. J., Sen, A., Roy, N., & Debnath, A. (2021). The soil phosphate fractionation fallacy. *Plant and Soil*, *459*, 1–11. https://doi.org/10.1007/s11104-020-04476-6

Beerling, D. J., Kantzas, E. P., Lomas, M. R., Wade, P., Eufrasio, R. M., Renforth, P., Sarkar, B., Andrews, M. G., James, R. H., Pearce, C. R., Mercure, J. F., Pollitt, H., Holden, P. B., Edwards, N. R., Khanna, M., Koh, L., Quegan, S., Pidgeon, N. F., Janssens, I. A., … Banwart, S. A. (2020). Potential for large-scale CO_2 removal via enhanced rock weathering with croplands. *Nature*, *583*, 242–248. https://doi.org/10.1038/s41586-020-2448-9

Beerling, D. J., Leake, J. R., Long, S. P., Scholes, J. D., Ton, J., Nelson, P. N., Bird, M., Kantzas, E., Taylor, L. L., Sarkar, B., Kelland, M., DeLucia, E., Kantola, L., Müller, C., Rau, G., & Hansen, J. (2018). Farming with crops and rocks to address global climate, food and soil security. *Nature Plants*, *4*, 138–147. https://doi.org/10.1038/s41477-018-0108-y

Bergmann, J., Weigelt, A., van der Plas, F., Laughlin, D. C., Kuyper, T. W., Guerrero-Ramirez, N., Valverde-Barrantes, O. J., Bruelheide, H., Freschet, G. T., & Iversen, C. M. (2020). The fungal collaboration gradient dominates the root economics space in plants. *Science Advances*, *6*(27), eaba3756. https://doi.org/10.1126/sciadv.aba3756

Bi, B. Y., Wang, Y., Wang, K., Zhang, H., Fei, H. Y., Pan, R. P., & Han, F. P. (2022). Changes in microbial metabolic C- and N-limitations in the rhizosheath and bulk soils along afforestation chronosequence in desertified ecosystems. *Journal of Environmental Management*, *303*, 114215. https://doi.org/10.1016/j.jenvman.2021.114215

Bi, B. Y., Yin, Q. L., & Hao, Z. Q. (2023). Root phosphatase activity is a competitive trait affiliated with the conservation gradient in root economic space. *Forest Ecosystems*, *10*, 100111. https://doi.org/10.1016/j.fecs.2023.100111

Buss, W., Hasemer, H., Ferguson, S., & Borevitz, J. (2023). Stabilisation of soil organic matter with rock dust partially counteracted by plants. *Global Change Biology*, *30*, e17052. https://doi.org/10.1111/gcb.17052

Cui, Y. X., Moorhead, D. L., Guo, X., Peng, S., Wang, Y., Zhang, X., & Fang, L. (2021). Stoichiometric models of microbial metabolic limitation in soil systems. *Global Ecology and Biogeography*, *30*(11), 2297–2311. https://doi.org/10.1111/geb.13378

Dai, Z., Liu, G., Chen, H., Chen, C., Wang, J., Ai, S., Wei, D., Li, D., Ma, B., Tang, C., Brookes, P. C., & Xu, J. (2019). Long-term nutrient inputs shift soil microbial functional profiles of phosphorus cycling in diverse agroecosystems. *The ISME Journal*, *14*(3), 757–770. https://doi.org/10.1038/s41396-019-0567-9

Du, E. Z., Terrer, C., Pellegrini, A. F. A., Ahlström, A., Lissa, C. J., Zhao, X., Xia, N., Wu, X. H., & Jackson, R. B. (2020). Global patterns of terrestrial nitrogen and phosphorus limitation. *Nature Geoscience*, *13*, 221–226. https://doi.org/10.1038/s41561-019-0530-4

Elias, M., Tanaka, M., Sakai, M., Toyama, H., Matsushita, K., Adachi, O., & Yamada, M. (2001). C-terminal periplasmic domain of *Escherichia coli* quinoprotein glucose dehydrogenase transfers electrons to ubiquinone. *Journal of Biological Chemistry*, *276*, 48356–48361. https://doi.org/10.1074/jbc.M107355200

Garcia, W. D., Amann, T., Hartmann, J., Karstens, K., Popp, A., Boysen, L. R., Smith, P., & Goll, D. (2020). Impacts of enhanced weathering on biomass production for negative emission technologies and soil hydrology. *Biogeosciences*, *17*(7), 2107–2133. https://doi.org/10.5194/bg-17-2107-2020

Goll, D. S., Ciais, P., Amann, T., Buermann, W., Chang, J. F., Eker, S., Hartmann, J., Janssens, I., Li, W., Obersteiner, M., Penuelas, J., Tanaka, K., & Vicca, S. (2021). Potential CO_2 removal from enhanced weathering by ecosystem responses to powdered rock. *Nature Geoscience*, *14*, 545–549. https://doi.org/10.1038/s41586-020-2448-9

Hagerty, S. B., Allison, S. D., & Schimel, J. P. (2018). Evaluating soil microbial carbon use efficiency explicitly as a function of cellular processes: Implications for measurements and models. *Biogeochemistry*, *140*(3), 269–283. https://doi.org/10.1007/s10533-018-0489-z

Han, M. G., Chen, Y., Li, R., Yu, M., Fu, L., Li, S., Su, J., & Zhu, B. (2022). Root phosphatase activity aligns with the collaboration gradient of the root economics space. *New Phytologist*, *234*, 837–849. https://doi.org/10.1111/nph.17906

Haque, F., Santos, R. M., Dutta, A., Thimmanagari, M., & Chiang, Y. W. (2019). Co-benefits of wollastonite weathering in agriculture: CO_2 sequestration and promoted plant growth. *ACS Omega*, *4*, 1425–1433. https://doi.org/10.1021/acsomega.8b02477

He, P., Zhang, Y. T., Shen, Q. R., Ling, N., & Nan, Z. B. (2023). Microbial carbon use efficiency in different ecosystems: A meta-analysis based on a biogeochemical equilibrium model. *Global Change Biology*, *29*(17), 4758–4774. https://doi.org/10.1111/gcb.16861

Hedley, M. J., Stewart, J., & Chauhan, B. (1982). Changes in inorganic and organic soil phosphorus fractions induced by cultivation practices and by laboratory incubations. *Soil Science Society of America Journal*, *46*, 970–976. https://doi.org/10.2136/sssaj1982.03615995004600050017x

Hou, E., Chen, C., Kuang, Y., Zhang, Y., Heenan, M., & Wen, D. (2016). A structural equation model analysis of phosphorus transformations in global unfertilized and uncultivated soils. *Global Biogeochemical Cycles*, *30*, 1300–1309. https://doi.org/10.1002/2016GB005371

Hou, E., Chen, C., Luo, Y., Zhou, G., Kuang, Y., Zhang, Y., Heenan, M., Lu, X., & Wen, D. (2018). Effects of climate on soil phosphorus cycle and availability in natural terrestrial ecosystems. *Global Change Biology*, *24*, 3344–3356. https://doi.org/10.1111/gcb.14093

IPCC. (2018). *IPCC special report on global warming of 1.5°C* (V. Masson-Delmotte, H. Pörtner, J. Skea, P. Zhai, D. Roberts, & P. R. Shukla, Eds.). Cambridge University Press.

Iversen, C. M. (2014). Using root form to improve our understanding of root function. *New Phytologist*, *203*(3), 707–709. https://doi.org/10.1111/nph.12902

Lambers, H. (2022). Phosphorus acquisition and utilization in plants. *Annual Review of Plant Biology*, *73*, 17–42. https://doi.org/10.1146/annurev-arplant-102720-125738

Lambers, H., Clode, P. L., Hawkins, H., Laliberté, E., Oliveira, R. S., Reddell, P., Shane, M. W., Stitt, M., & Weston, P. (2015). Metabolic adaptations of the non-mycotrophic Proteaceae to soils with low phosphorus availability. In W. C. Plaxton & H. Lambers (Eds.), *Annual plant reviews, vol. 48: Phosphorus metabolism in plants* (pp. 289–336). Wiley & Sons. https://doi.org/10.1002/9781118958841.ch11

Lambers, H., Hayes, P. E., Laliberté, E., Oliveira, R. S., & Turner, B. L. (2015). Leaf manganese accumulation and phosphorus-acquisition efficiency. *Trends in Plant Science*, *20*(2), 83–90. https://doi.org/10.1016/j.tplants.2014.10.007

Li, X. W., Zhang, C. L., Zhang, B. B., Wu, D., Zhu, D. D., Zhang, W., Ye, Q., Yan, J. H., Fu, J. M., Fang, C. L., Hua, D. L., & Fu, S. L. (2020). Nitrogen deposition and increased precipitation interact to affect fine root production and biomass in a temperate forest: Implications for carbon cycling. *Science of the Total Environment*, *765*, 144497. https://doi.org/10.1016/j.scitotenv.2020.144497

Liu, Y., Zhang, G. H., Luo, X. Z., Hou, E. Q., Zheng, M. H., Zhang, L. L., He, X. J., Shen, W. J., & Wen, D. Z. (2021). Mycorrhizal fungi and phosphatase involvement in rhizosheath phosphorus transformations improves plant nutrition during subtropical forest succession. *Soil Biology and Biochemistry*, *153*, 108099. https://doi.org/10.1016/j.soilbio.2020.108099

Lu, J. L., Jia, P., Feng, S. W., Wang, Y. T., Zheng, J., Ou, S. N., Wu, Z. H., Liao, B., Shu, W. S., Liang, J. L., & Li, J. T. (2022). Remarkable effects of microbial factors on soil phosphorus bioavailability: A country-scale study. *Global Change Biology*, *16213*, 4459–4471.

Ma, Z. Q., Guo, D. L., Xu, X. L., Lu, M. Z., Bardgett, R. D., Eissenstat, D. M., McCormack, M. L., & Hedin, L. O. (2018). Evolutionary history resolves global organization of root functional traits. *Nature*, *555*(7694), 94–97. https://doi.org/10.1038/nature25783

Manzoni, S., Čapek, P., Mooshammer, M., Lindahl, B. D., Richter, A., & Šantrůčková, H. (2017). Optimal metabolic regulation along resource stoichiometry gradients. *Ecology Letters*, *20*(9), 1182–1191. https://doi.org/10.1111/ele.12815

Manzoni, S., Taylor, P., Richter, A., Porporato, A., & Agren, G. I. (2012). Environmental and stoichiometric controls on microbial carbon-use efficiency in soils. *New Phytologist*, *196*(1), 79–91. https://doi.org/10.1111/j.1469-8137.2012.04225.x

Mersi, W. V., Kuhnert-Finkernagel, R., & Schinner, F. (1992). The influence of rock powders on microbial activity of three forest soils. *Zeitschrift für Pflanzenernährung und Bodenkunde*, *155*(1), 29–33. https://doi.org/10.1002/jpln.19921550107

Pang, J., Ruchi, B., Zhao, H., Bansal, R., Bohuon, E., Lambers, H., Ryan, M. H., Ranathunge, K., & Siddique, K. M. H. (2018). The carboxylate-releasing phosphorus-mobilising strategy could be proxied by foliar manganese concentration in a large set of chickpea germplasm under low phosphorus supply. *New Phytologist*, *219*, 518–529. https://doi.org/10.1111/nph.15200

Paradelo, R., Oort, F., Barré, P., Billiou, D., & Chenu, C. (2016). Soil organic matter stabilization at the pluri-decadal scale: Insight from bare fallow soils with contrasting physicochemical properties and macrostructures. *Geoderma*, *275*, 48–54. https://doi.org/10.1016/j.geoderma.2016.04.009

Parfitt, R. L. (1979). The availability of P from phosphate-goethite bridging complexes. Desorption and uptake by ryegrass. *Plant and Soil*, *53*, 55–65. https://doi.org/10.1007/BF02181879

Peña-Ramírez, V. M., Vázquez-Selem, L., & Siebe, C. (2009). Soil organic carbon stocks and forest productivity in volcanic ash soils of different age (1835–30,500 years B.P.) in Mexico. *Geoderma*, *149*, 224–234. https://doi.org/10.1016/j.geoderma.2008.11.038

Pregitzer, K. S., DeForest, J. L., Burton, A. J., Allen, M. F., Ruess, R. W., & Hendrick, R. L. (2002). Fine root architecture of nine North American trees. *Ecological Monographs*, *72*(1), 293–309. https://doi.org/10.1890/0012-9615(2002)072[0293:FRAONN]2.0.CO;2

Reith, F., Zammit, C. M., Pohrib, R., Gregg, A. L., & Wakelin, S. A. (2015). Geogenic factors as drivers of microbial community diversity in soils overlying polymetallic deposits. *Applied and Environmental Microbiology*, *81*(22), 7822–7832. https://doi.org/10.1128/aem.01856-15

Renforth, P., & Henderson, G. (2017). Assessing ocean alkalinity for carbon sequestration. *Reviews of Geophysics*, *55*(3), 636–674. https://doi.org/10.1002/2016RG000533

Rodríguez, H., Fraga, R., Gonzalez, T., & Bashan, Y. (2006). Genetics of phosphate solubilization and its potential applications for improving plant growth-promoting bacteria. *Plant and Soil*, *287*, 15–21. https://doi.org/10.1007/s11104-006-9056-9

Sanchez, G., Trinchera, L., Sanchez, M. G., & FactoMineR, S. (2013). *Package 'plspm'*. Citeseer.

Sinsabaugh, R. L., & Follstad Shah, J. J. (2012). Ecoenzymatic stoichiometry and ecological theory. *Annual Review of Ecology, Evolution, and Systematics*, *43*, 313–343. https://doi.org/10.1146/annurev-ecolsys-071112-124414

Sinsabaugh, R. L., Turner, B. L., Talbot, J. M., Waring, B. G., Powers, J. S., Kuske, C. R., Moorhead, D. L., & Follstad Shah, J. J. (2016). Stoichiometry of microbial carbon use efficiency in soils. *Ecological Monographs*, *86*(2), 172–189. https://doi.org/10.1890/15-2110.1

Smith, P., Adams, J., Beerling, D. J., Beringer, T., Calvin, K. V., Fuss, S., Griscom, B., Hagemann, N., Kammann, C., Kraxner, F., Minx, J. C., Popp, A., Renforth, P., Vicente, J. L. V., & Keesstra, S. (2019). Land-management options for greenhouse gas removal and their impacts on ecosystem services and the sustainable development goals. *Annual Review of Environment and Resources*, *44*, 255–286. https://doi.org/10.1146/annurev-environ-101718-033129

Smith, P., Davis, S. J., Creutzig, F., Fuss, S., Minx, J., Gabrielle, B., Kato, E., Jackson, R. B., Cowie, A., Kriegler, E., van Vuuren, D. P., Rogelj, J., Ciais, P., Milne, J., Canadell, J. G., McCollum, D., Peters, G., Andrew, R., Krey, V., … Yongsung, C. (2016). Biophysical and economic limits to negative CO_2 emissions. *Nature Climate Change*, *6*, 42–50. https://doi.org/10.1038/nclimate2870

Tao, F., Huang, Y. Y., Hungate, B. A., Manzoni, S., Frey, S. D., Schmidt, M. W. I., Reichstein, M., Carvalhais, N., Ciais, P., Jiang, L. F., Lehmann, J., Wang, Y. P., Houlton, B. Z., Ahrens, B., Mishra, U., Hugelius, G., Hocking, T. D., Lu, X. J., Shi, Z., … Luo, Y. Q. (2023). Microbial carbon

use efficiency promotes global soil carbon storage. *Nature*, *618*, 981–985. https://doi.org/10.1038/s41586-023-06042-3

Terrer, C., Jackson, R. B., Prentice, I. C., Keenan, T. F., Kaiser, C., Vicca, S., Fisher, J. B., Reich, P. B., Stocker, B. D., Hungate, B. A., Peñuelas, J., McCallum, I., Soudzilovskaia, N. A., Cernusak, L. A., Talhelm, A. F., Sundert, K. V., Piao, S. L., Newton, P. C. D., Hovenden, M. J., … Franklin, O. (2019). Microbial carbon use efficiency in different ecosystems: Nitrogen and phosphorus constrain the CO_2 fertilization of global plant biomass. *Nature Climate Change*, *9*, 684–689. https://doi.org/10.1038/s41558-019-0545-2

Treseder, K. K., & Allen, M. F. (2002). Direct nitrogen and phosphorus limitation of arbuscular mycorrhizal fungi: A model and field test. *New Phytologist*, *155*(3), 507–515. https://doi.org/10.1046/j.1469-8137.2002.00470.x

Trouvelot, A., Kough, J. L., & Gianinazzi-Pearson, V. (1986). Mesure du taux de mycorhization VA d'un systeme radiculaire. Recherche de methods d'estimation ayant une signification fonctionnelle. In V. Gianinazzi-Pearson & S. Gianinazzi (Eds.), *Physiological and genetical aspects of mycorrhizae* (pp. 217–221). INRA.

Turner, B. L. (2008). Resource partitioning for soil phosphorus: A hypothesis. *Journal of Ecology*, *96*(4), 698–702. https://doi.org/10.1111/j.1365-2745.2008.01384.x

Vitousek, P. M., Porder, S., Houlton, B. Z., & Chadwick, O. A. (2010). Terrestrial phosphorus limitation: Mechanisms, implications, and nitrogen–phosphorus interactions. *Ecological Applications*, *20*(1), 5–15. https://doi.org/10.1890/08-0127.1

Wen, Z. H., Li, H., Shen, Q., Tang, X. M., Xiong, C. Y., Li, H. G., Pang, J. Y., Ryan, M. H., Lambers, H., & Shen, J. B. (2019). Tradeoffs among root morphology, exudation and mycorrhizal symbioses for phosphorus–acquisition strategies of 16 crop species. *New Phytologist*, *223*, 882–895. https://doi.org/10.1111/nph.15833

Wen, Z. H., White, P. J., Shen, J. B., & Lambers, H. (2022). Linking root exudation to belowground economic traits for resource acquisition. *New Phytologist*, *233*, 1620–1635. https://doi.org/10.1111/nph.17854

Yan, Y. X., Dong, X. H., Li, R. S., Zhang, Y. K., Yan, S. K., Guan, X., Yang, Q. P., Chen, L. C., Fang, Y. T., Zhang, W. D., & Wang, S. L. (2023). Wollastonite addition stimulates soil organic carbon mineralization: Evidences from 12 land-use types in subtropical China. *Catena*, *225*, 107031. https://doi.org/10.1016/j.catena.2023.107031

SUPPORTING INFORMATION

Additional supporting information can be found online in the Supporting Information section at the end of this article.

How to cite this article: Bi, B., Li, G., Goll, D. S., Lin, L., Chen, H., Xu, T., Chen, Q., Li, C., Wang, X., Hao, Z., Fang, Y., Yuan, Z., & Lambers, H. (2024). Enhanced rock weathering increased soil phosphorus availability and altered root phosphorus-acquisition strategies. *Global Change Biology*, *30*, e17310. https://doi.org/10.1111/gcb.17310